Modeling, Simulation and Comparison Study of Cirrus Clouds' Ice Crystals

Jorge M. Villa[*a], Sandra L. Cruz-Pol[*a], José Colom-Ustáriz[*a], Stephen M. Sekelsky[** b]

[a]Dept. of Electrical and Computer Engineering, Univ. of Puerto Rico/Mayagüez Campus
[b]Microwave Remote Sensing Laboratory, Univ. of Massachusetts/Amherst

ABSTRACT

Various methods and techniques to estimate ice crystals radar response have been developed to study the structure of cirrus clouds. Most methods assume a spherical shape for the ice crystals. This assumption leads to mistakes on the parameter estimation related to the particles' size. In this work, we modeled the shape of ice particles found in cirrus cloud as measured by airborne instruments, specifically ice bullets. These can be found depending on the temperature and cloud altitude, isolated or in groups of two or more bullets, called bullet rosettes. The model of the bullet rosettes was developed using the parameters obtained by airborne measurements from the National Center for Atmospheric Research (NCAR). These measurements were done by Video Ice Particle Sampler (VIPS). This is an airborne instrument that flies inside cirrus clouds, and takes samples of the cirrus cloud particles sizes up to 5 μm in size. With these sample parameters we modeled the actual shape of the bullet rosettes using the software DDSCAT. This software allows us to create irregular models of particles using the Discrete Dipole Approximation method. With this model we are able to analyze the backscattering produced by the bullets rosettes model or reflectivity and compute the total volume backscattering coefficient expected from the cirrus clouds. Different models of ice crystals' size are compared, some assume constant ice density through out the bullet, while others used the density as a function of the dimension of the bullet.

1. INTRODUCTION

Cirrus clouds play an important roll on the balance of earth's energy dynamics, therefore affecting climate systems[1]. In addition, they indirectly affect the study of other systems such as marine and dessert surfaces, and therefore the necessity of studying and estimating their macrophysics characteristics such as density, dimensions, and layer constitution[2]. To achieve this, we need knowledge of their microphysics characteristics such as ice water content, (IWC), crystal size distribution and crystals' shape[3], because these dictate the clouds' radiative properties. Studies show that radars operating at frequencies smaller than 12 GHz have obtain successful estimates of the microphysical properties from precipitating clouds and other clouds with high content of liquid water, however when these were used in cirrus clouds, these radars did not obtain good estimates[4]. Millimeter wave radar has proven to be sensitive at studying particles smaller than 1mm[5-7]. When operated at frequencies near the atmospheric windows (35, 94, 140, and 220 GHz) the millimeter wave radar can be useful to study the microphysical properties of the clouds[5, 8].

As the research from Schneider and Stephens demonstrate, we can use Rayleigh approximation when we analyze the backscattering from ice modeled particles as spheres with signals near 33 GHz. But when studying the scattering from particles larger than 0.6mm, with frequency signals greater or equal than 95GHz, Rayleigh approximation not longer holds since the wavelength are comparable with the particles' size[9]. This fact motivated several studies that compute and analyze the scattering of different ice crystal shapes.

Evans and Vivekanandan[10] started to simulate the radar reflectivity and the upwelling microwave brightness temperature of cloud's crystals to derive its microphysical parameters, observing that the results were dependent on the shape, size and other microphysical properties. Simulations from the electromagnetic scattering of the ice particles using the Discrete Dipole Approximation (DDA), assuming hexagonal plates and columns, use constant values for the bulk density (0.92 g/cm^3), index of refraction (at –20ºC; m= 1.784 – j0.0016 for 37 GHz), and others. On this study, it was found that the results were dependent on these values, previously assumed constant, mostly on the bulk density. Dungey and Bohren[11] analyzed the backscattering produced by the ice particles with a 94 GHz signal at different angles and with vertical polarization using the Coupled-Dipole Method, with the same principle as the DDA. They assumed a constant index of refraction of 1.878 + j0.000476 for a temperature of 0ºC, and used the hexagonal prismatic as the shape for the ice crystals. Finally, they found that the backscattering varies considerable with respect to the angle of incident of the signal, but that changes in the polarization do not have considerable effects

Tang and Aydin[12-14], performed scattering studies of the ice at 94 and 220 GHz using the Finite Difference Time Domain (FDTD) method to simulate the scattering of the ice crystals. The geometric models of the crystals were given by Auer and Veal[15] as hexagonal plate, stellar crystal and the hexagonal column. For the three models a constant ice density of 0.9 g cm^{-3}, constant permittivity of 3.1307 – j0.0047 and 3.1307 – j0.0047 were assumed, for 94 and 220 GHz, respectively[16-17]. The study was performed for ice crystals sizes between 100 and 200 μm. Different scattering characteristics among the shapes analyzed were found when observing the dual frequency ratio (DFR). In addition, the linear depolarization ratio versus elevation angle was found to be similar for the stellar crystals and the hexagonal plates, and significantly different for the columns. It was concluded that the ice crystals observations at different elevation angles can be used to discriminate between the plates and columns efficiently.

Sekelsky et al.[18-19] used simulations from the ice crystals backscattering at various millimeter wavelengths using the DDA models on the version 5ª of DDSCAT, assuming a model based in a gamma distribution and using a more realistic density model where ice density is not constant, as in previous studies, but decreases with the particles' diameter. They calculated the dual-wavelength ratio (DWR) and used it to train a neural network, to obtain iteratively estimates of the particle size and number concentration, N_0, until a reasonably small error was achieved. Their findings also agree with previous studies where the shape and orientation are the principal causes of error on the DWR estimates and other products.

There are few studies that consider the shape of the bullet and the bullet rosette, e.g., Aydin and Walsh[20-21]. They made simulations implementing the geometric shape of the bullet and bullet rosette estimated by Heymsfield[22] for a temperature range between –18 y –20 ºC, but, they continued using a constant density of 0.9 g cm^{-3}, appropriate for temperatures between –9.3 to –3.5 ºC.

The work presented here, specifically analyzes crystals with bullet and bullet rosettes shapes, because previous studies have shown that these two forms are the most common in cirrus clouds[23-24]. To create a model with the real shape of the ice crystals, we use data obtained form the National Center for Atmospheric Research (NCAR). In addition, we use a more realistic density function that varies with the longitude of the bullet, therefore we need to compute the indexes of refraction for every longitude and frequency. Then, we simulate their respective backscattering for the 33 and 95 GHz, analyzing the corresponding dual wavelength ratio, DWR.

2. BULLET AND BULLETS ROSETTES MODELS

The ice particle's models will be estimated using the measured parameters of the particle's shape given by A. Heymsfield from the National Center for Atmospheric Research (NCAR).[24] Measurements were collected with the Video Ice Particle Sampler (VIPS). This is an airborne instrument that flies inside cirrus clouds, and takes samples of the cirrus cloud particles sizes up to 5 μm in size. The VIPS have an electro-optical and imaging unit that is in charge of collecting data, and another part designated to record data. The particles' images are recorded in two formats, one is at 30 Hz on high-resolution Hi-8 VCRs, the other format is at 1 Hz, digitized in real-time in an Apple PowerPC[25].

Various shapes of the bullet rosettes are observed (see Fig. 1). The angles among the bullets within the rosette are random between 70° y 90°. Each bullet has a longitude relation, L (mm), versus wide, w (mm), (twice times the apothem) for temperatures between –18 y –20 ºC[26]

Bullet with $L \leq 0.3$ mm

$$w = 0.25L^{0.7856} \quad (\text{mm}) \tag{1}$$

Bullet with $L \geq 0.3$ mm

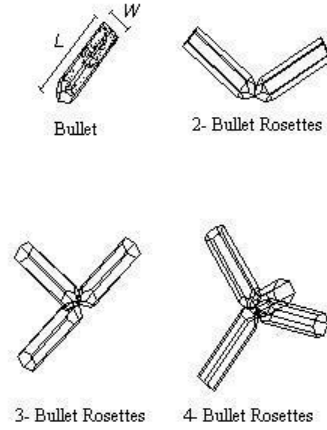$$w = 0.185L^{0.532} \quad (\text{mm}) \tag{2}$$

Fig. 1: Bullet and Bullet Rosettes with different angles of junction

In this way the equations were determined for the bulk density, ρ, of the bullet rosettes, considering the solid ice density as 0.9 g cm⁻³ and using the volume of ice in individual crystals[26]

$$\rho = 0.78L^{0.0038} \quad (\text{g cm}^{-3}) \tag{3}$$

As the Wiener's theorem states in[27], the complex index of refraction, m, depends of the bulk density when dealing with ice dry particles:

$$m = \frac{2 + n_i^2 + 2f_j\left(n_i^2 - 1\right)}{2 + n_i^2 + f_i\left(-n_i^2 + 1\right)} \tag{4}$$

where f_i represents an adimensional fraction of the volume of air and ice and it is defined as:

$$f_i = \frac{\rho}{\rho_i} \tag{5}$$

with ρ_i as the solid ice density (0.9 g cm⁻³) and where n_i is the complex index of refraction of solid ice which is different for every frequency (33 and 95 GHz)[28-29]. Using the above equations, we will obtain an index of refraction for each frequency and each bullet size.

3. SIMULATION FROM BULLET AND BULLETS ROSETTES

3.1 DDSCAT Program

In this work, we used the DDSCAT software to compute the backscattering produced by ice crystals. This program is based on the discrete-dipole approximation method, DDA, which is a very efficient tool to calculate parameters such as Mie scattering and absorption from particles with irregular geometric shapes and complex refractive index. This software includes some predetermined geometric shapes such as spheres, hexagon plates, prisms, rectangles, and others. Besides, it has a toolbox that can be used to design any geometric shape desired[30-31]. The DDA method approximates the object geometry by means of a polarizable dipoles array; DDSCAT distributes these dipoles on a cubic lattice Fig. 2.

Although DDA can describe any geometry, it is limited by a minimum distance d that should exist between dipole. This distance should be inversely proportional to any structural longitude on the target and to the wavelength. Previous studies[32] sum up the two criteria in equation 6.

$$|m|kd < 0.5 \qquad (6)$$

with m as the complex refractive index of the object material, and k as the wavenumber of the surrounding medium.

Another factor that should be considered is the number of dipoles that describes the target. For each dipole an electric field is calculated, and at the end the sum of all the fields due to each dipole will be the total electric field, from which the backscattering coefficient will be computed and other products as the absorption and scattering coefficient factors. In order to obtain more accurate results, we should work with a large number of dipoles. This implies more computational time. An increment on the target's size should be contra rested with an increase on the number of dipoles.
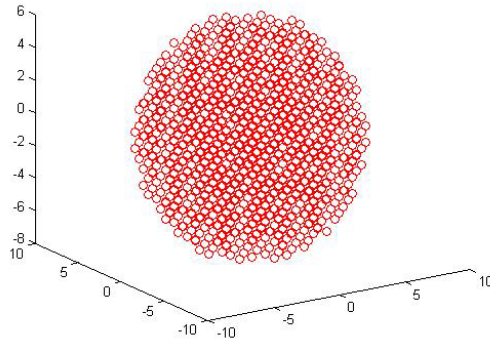

Fig. 2: Polarizable dipoles array over a cubic lattice describing a sphere

3.2 Bullet and Bullet Rosettes Toolbox for DDSCAT Program

We developed two toolboxes for DDSCAT where we implemented the most common shapes of the cirrus ice crystals, i.e. the bullet and bullet rosettes. Using a single DDSCAT environment by means of the *ddscat.par* file[31], we specified which one of the geometry we wanted to use and parameters such as size, dielectric constant of the material, and in general all the parameters related to the target to be analyzed. Several routines were modified from the original DDSCAT program. These two subroutines were developed by implementing the bullet and bullet rosettes models previously obtained from the NCAR data.

The two subroutines expect the longitude of the bullet, the apothem from the base of the hexagonal bullet, the maximum number of dipoles that can be used to describe the bullet, as well as the number of bullets inside the bullet rosette, which are given by DDSCAT that at the same time loads the *ddscat.par* file. Next, the subroutine starts creating an array of dipoles depending on the initial dimensions and iteratively testing to verify that the dipoles are inside the bullet's volume and that the criteria of the dipole spacing is preserved (see Fig. 3). Finally, the subroutine delivers to the main DDSCAT program a matrix with the positions of the dipoles that describes the bullet, and with other general subroutines, the scattering coefficient and other products are computed.
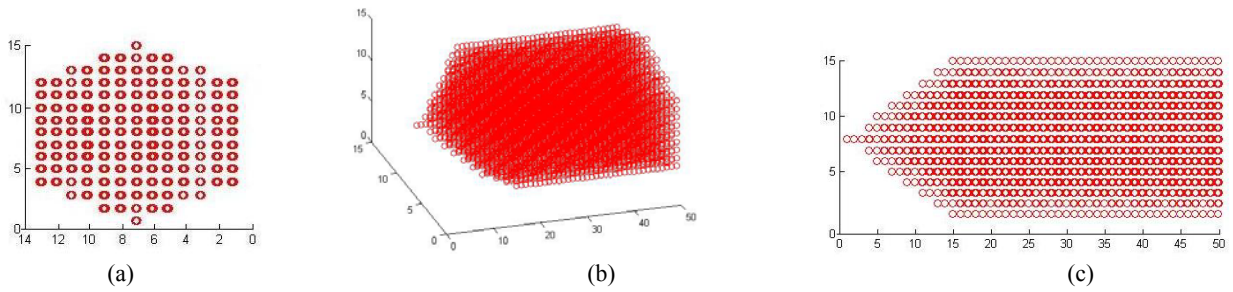
Fig. 3: Bullet formed by a dipole array separated by distance *d* (coordinate/*d*) (a) top view, (b) 3D-view, (c) side view
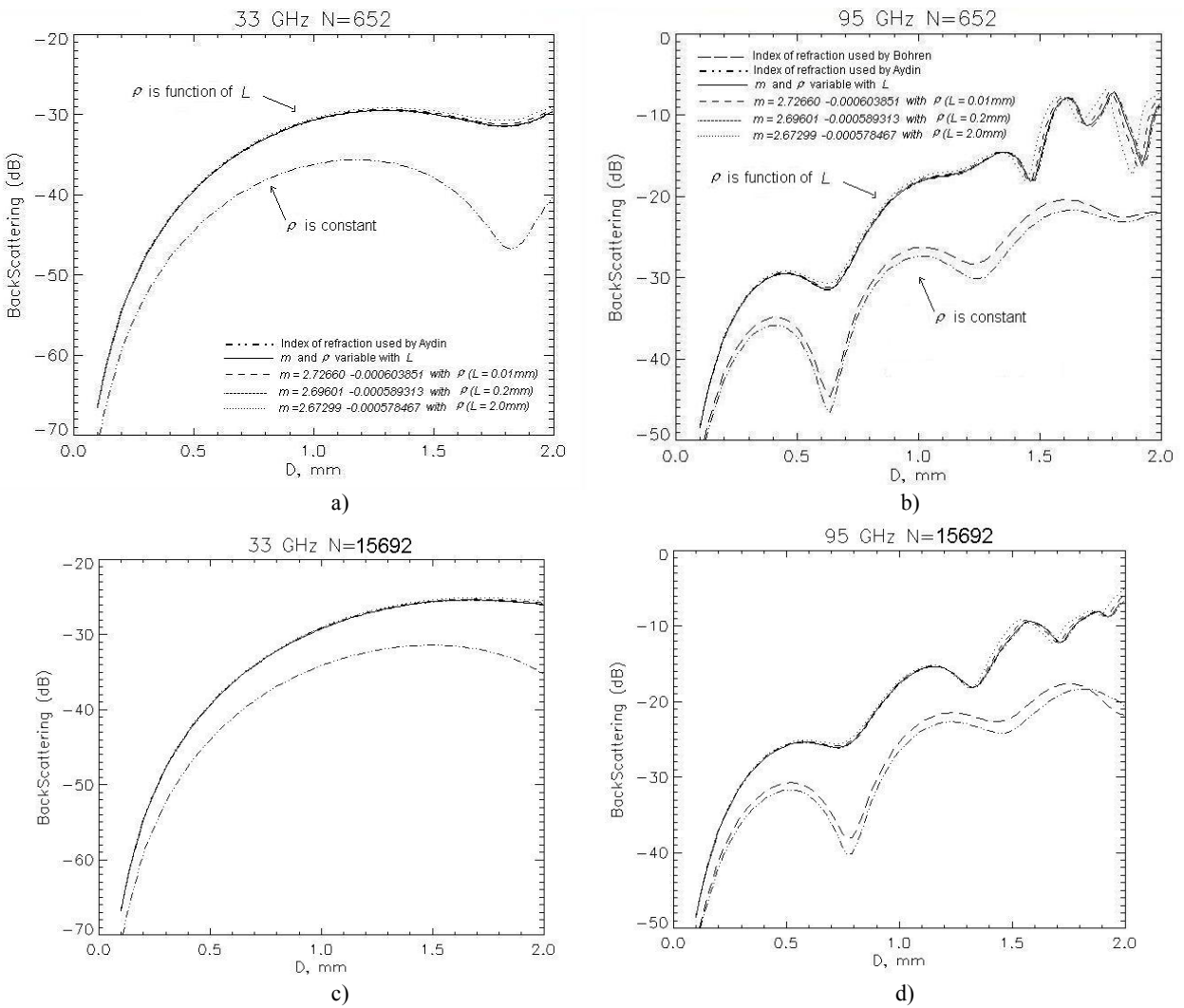

Fig. 4: Backscattering (10 logσ_b) of different indexes of refraction, a) Backscattering in dB to 33GHz with 652 dipoles array, b) Backscattering in dB to 95GHz with 652 dipoles array, c) Backscattering in dB to 33GHz with 15692 dipoles array, d) Backscattering in dB to 95GHz with 15692 dipoles array. Figure 4(a-d) the top traces are for density as a function of *L*, and the bottom group of traces is given with ρ constant.

4. BACKSCATTERING AND DWR ANALYZE WITH IDL PROGRAM AND DDSCAT

Once the bullet toolbox was created in DDSCAT, we proceeded to use it to simulate the crystal's backscattering at 33 and 95 GHz. Figure 4 shows the backscattering for the bullet crystal of different sizes using several models for index of refraction and crystal density. The figure shows the sensitivity of the backscattering to the index of refraction, showing the necessity of considering the index of refraction for each size and density of the ice crystal, and not assuming a constant density for all the bullets sizes.

It can also be seen that the backscattering obtained when varying the index of refraction according to the particle size is not significantly different to the results obtained when using constant indexes of refraction for different particle sizes. But these constant indexes of refraction must be related with the density function for the bullet rosette, and with a range of sizes between 0.01- 5 mm. By other way, methods assuming a constant density, or other ice crystal shape affect the obtained backscattering because the index of refraction obtained in this way is not representative of the dynamics of the bullet rosette.

To study the effect of the selection of number of dipoles, we defined the ratio of the backscattering coefficient at two distinct crystal lengths, i.e., L_h=1.8mm and L_l=1.0mm. These values were chosen for their contrasting backscattering coefficients.

$$\text{Backscattering Ratio} = \frac{\xi(L_h)}{\xi(L_l)} \qquad (7)$$

The purpose is to see how the shape of the Mie backscattering function (as those in Fig. 4) changes with the number of dipoles, N, used in DDscat code. Under ideal conditions, this ratio should be constant. We start with N =128, since this is the lowest limit that complies with DDSCAT requirements for dipole separation, and we increase this number until N=16,000. The ratio was computed for each N and plotted below (see Fig. 5).
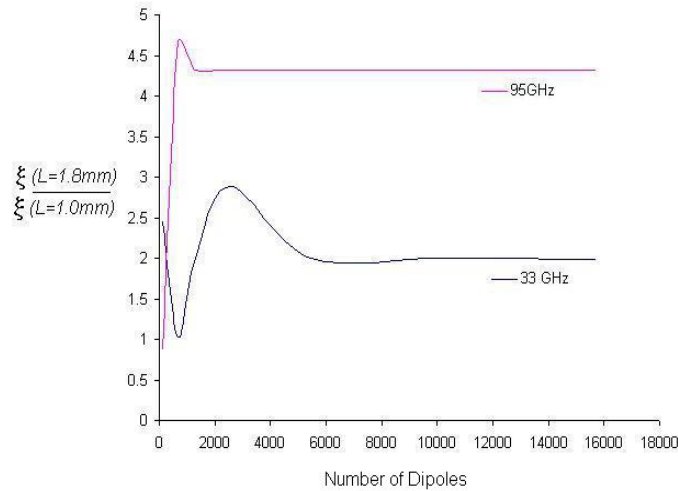

Fig. 5. Ratio between two points of backscattering coefficient for different dipole numbers

We chose to use 15692 dipoles to be extra conservatives, but in reality we can use less dipoles (approximately 6,000). Using less dipoles we can save computing time considerably. The computing time using 15692 dipoles is approximately 5 hours using an IBM Intellistation Z Pro Type 6866, Pentiun 3 with 392,624 KB RAM.

Given that one of the objectives is to analyze the DWR, we designed an interface between DDSCAT and IDL program. We developed a routine that iteratively collects data from IDL such as the index of refraction, m, which is computed according to the particles size and the index of refraction of the solid ice, n_i, and saving m in DDSCAT to compute the backscattering and again this value is saved in IDL to obtain the DWR.

The DWR is defined as[18]

$$DWR = 10\log\left(\frac{\lambda_l^4 |K_I(\lambda_h)|^2 \int_0^\infty \xi_b(D,\lambda_l,\rho)D^{(2+\mu)}e^{\left[-(3.67+\mu)\frac{D}{D_0}\right]}dD}{\lambda_h^4 |K_I(\lambda_l)|^2 \int_0^\infty \xi_b(D,\lambda_h,\rho)D^{(2+\mu)}e^{\left[-(3.67+\mu)\frac{D}{D_0}\right]}dD}\right) \qquad (8)$$

where λ_l y λ_h are the values of the smaller wavelength and greater respectively, K_I is an dimensionless quantity that depends on the index of refraction and on the density. For ice we assumed 0.176 for both frequencies. The backscattering, ξ_b, for both frequencies is given by DDSCAT and this one depends on the target's diameter, D, which is the longitude of the bullet, L. The parameter μ describes the order of the gamma distribution and can be values between 2 and - 2[33].
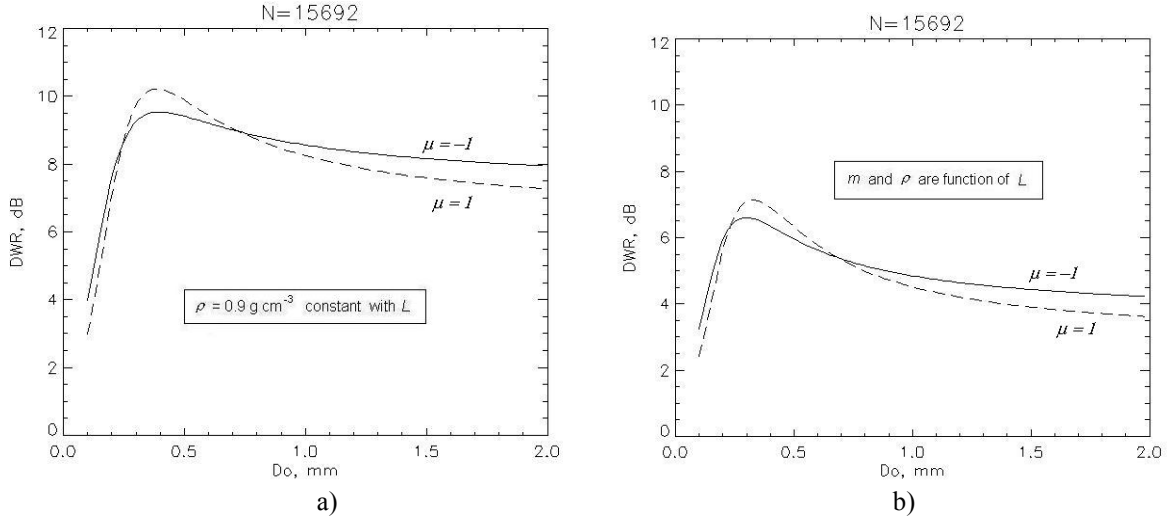

Fig. 6: DWR from the bullet rosette. Both plots were calculated using 15,692 dipoles for the DDScat code.
a) Index of refraction and bulk density used by Aydin, b) Index of refraction and density in function of crystal length

5. CONCLUSIONS

Analyzing the backscattering at 33 and 95 GHz simulated in IDL and implementing a more realistic model of the ice crystals density function we found that for a range between $0.01 – 2$ mm, negligible changes can be found when varying the index of refraction. Depending on the ice crystal size, we can obtain satisfactory results assuming a constant index of refraction derived from the realistic ice crystal density function. Significative changes were found when using density models that do not correspond to the natural condition of the ice crystals such as shape, temperature and height obtaining the principal variation when using a density model of 9 g cm^{-3} because this model does not correspond to the typical shape nor the temperature of the bullet rosette nor the height. It was found that the density has a big effect in the ice crystals backscattering. Compiling with the software criteria used for the computation of the backscattering is and important factor. Consistent results were found when using 2056 or more dipoles.

ACKNOWLEDGEMENTS

REFERENCES

1. G. L. Stephens, S. C. Tsay, P. W. Stackhouse Jr., and P. J. Flatau, "The relevance of the microphysical and radiative properties of cirrus clouds to climate and climatic feedback," *J. Atmos. Sci.,* **47**, pp. 1742-1753, 1990.
2. E. O. Schmidt, D. P. Kratz, B. A. Wielicki, "Effects of cirrus clouds and the atmosphere over land and ocean surfaces," *Proceedings of IGARSS 93 IEEE,* vol. 3, pp. 1107-1112, 1993.
3. H. Lemke, M. Quante, O. Danne, and E. Raschke, "The Role of Ice Particle Shape and Size Distributions in Polarimetric Radar Measurands at 95 GHz," *Proceedings of IGARSS 99 IEEE,* **1**, pp. 149-151, 1999.
4. E. E. Clothiaux, M. A. Miller, B. A. Albrecht, T. P. Ackerman, J. Verlinde, D. M. Babb, R. M. Peters and W. J. Syrett, "An evaluation of a 94 GHz radar for remote sensing of cloud properties," *J. Atmos. Ocean. Technol.*, **12**, no. 2, pp. 201-229, 1995.
5. R. Lhermitte, "A 95 GHz doppler radar of cloud observations," *J. Atmos. Ocean. Technol.*, **4**, pp. 36-48, 1987.
6. S. M. Sekeslky, and R. E. McIntosh, "Cloud Observations with a Polarimetric 33 GHz and 95 GHz radar," *Meteor. Atmos. Phys.*, vol. 58, pp. 123-140, 1996.
7. S. Y. Matrosov, "Radar reflectivity in snowfall," *IEEE. Trans. Geosci. Remote. Sens.*, **30**, pp. 454-461, 1992.
8. R. J. Doviak, and D. S. Zrnic, *Doppler Radar and Weather Observations*, Chapter 8, Second edition, 1993 Academic Press.
9. T. L. Schneider and G. L. Stephens, "Theoretical aspects of modeling backscattering by cirrus ice particles at millimeter wavelengths," *J. Atmos. Sci.*, **52**, no. 23, pp. 4367-4385, 1995
10. K. F. Evans and J. Vivekanandan, "Multiparameter radar and microwave radiative transfer modeling of nonspherical atmospheric ice particles," *IEEE Trans. Geosci. Remote Sensing.,* **28**, pp. 423-437, July 1990
11 C. E. Dungey and C. F. Bohren, "Backscattering by nonspherical hydrometeors as calculated by the coupled-dipole method: An application in radar meteorology," *J. Atmos. Ocean. Technol.*, **10**, pp. 526-532, 1993.
12 C. Tang and K. Aydin, "Scattering from ice at 94 and 220 GHz millimeter wave frequencies," *IEEE Trans. Geosci. Remote Sens.,* **33**, pp. 93-99, 1995.
13 K. Aydin and C. Tang, "Millimeter wave radar scattering from model ice crystal distributions," *IEEE Trans. Geosci. Remote Sens.,* **35**, pp. 140-146, 1997.
14 K. Aydin and C. Tang, "Relationship between IWC and polarimetric radar measurement at 94 and 220 GHz for hexagonal columns and plates," *J. Atmos. Ocean. Technol.*, **14**, pp. 1055-1063, 1997.
15 A. H. Auer and D. L. Veal, "The dimensions of ice crystals in natural clouds," *J. Atmos. Sci.*, **27**, pp. 919-926, 1970
16 P. S. Ray, "Broadband complex refractive indices of ice and water," *Appl. Opt.,* **11**, pp. 1836-1844, 1972
17 C. F. Bohren and L. J. Battan, "Radar backscattering of microwaves by spongy ice spheres," *J. Atmos. Sci.*, **39**, pp. 2623-2628, 1982
18 S. M. Sekelsky, W. L. Ecklund, J. M. Firda, K. S. Gage, R. E. McIntosh, "Particle Size Estimation in Ice-Phase Clouds Using Multifrequency Radar Reflectivity Measurements at 95, 33 and 2.8 GHz," *J. Appl. Meteor.*, **38,** pp. 5-27, 1999.
19 S. M. Sekelsky, R. E. McIntosh, W. L. Ecklund, K. S. Gage, 1998: Ice Crystal Size Estimation Using Multiple-wavelength Radar. *Geoscience and Remote Sensing Symposium Proceedings. IGARSS '98.*, **1**, 425 -428
20 K. Aydin and T. M. Walsh, "Computational study of millimeter wave scattering from bullet rosette type ice crystals," *Geoscience and Remote Sensing Symposium Proceedings. IGARSS '96.*, **1**, pp. 563-565, 1996.
21 K. Aydin and T. M. Walsh, "Millimeter wave scattering from spatial and planar bullet rosettes," *IEEE. Trans. Geosci. Remote. Sens.,* **37**, pp. 1138-1150, 1999.
22 A. J. Heymsfield and R. G. Knollenberg, "Properties of cirrus generating cells," *J. Atmos. Sci.*, **29**, pp. 1358-1366, 1972.
23. D. L. Mitchell, and W. P. Arnott, "A model predicting the evolution of ice particle size spectra and radiative properties of cirrus clouds-Part II: Dependence of absorption and extinction on ice crystal morphology," *J. Atmos. Sci.*, **51**, no. 6, pp. 817-832, 1994

24 A. J. Heymsfield and C. M. R. Platt, "A Parameterization of the Particle Size Spectrum of Ice Clouds in Terms of the Ambient Temperature and Ice Water Content," *J. Atmos. Sci.*, **41**, pp. 846-855, 1984

25. A. J. Heymsfield, " www.atd.ucar.edu/dir_off/airborne/visp.html, " 2000.

26 A. J. Heymsfield, "Ice crystal terminal velocities," *J. Atmos. Sci.*, **29**, pp. 1348-1357, 1972

27 T. Oguchi, "Electromagnetic wave propagation and scattering in rain and other hydrometeors," *Proc. IEEE,* **71**, pp. 1029-1078, 1983

28 P. Ray, "Broadband comples refractive indices of ice and water," *Appl. Opt.,* **11**, pp. 1836-1844, 1972.

29 S. G. Warren, "Optical constants of ice from the ultraviolet to the microwave," *Appl. Opt.,* **25**, pp. 1206-1225, 1984.

30. B. T. Draine and P. J. Flatau, "Discrete-dipole approximation for scattering calculations," *J. Opt. Soc. Am. A*, **11**, pp. 1491-1499, 1994.

31. B. T. Draine and P. J. Flatau, *User Guide to the discrete dipole approximation code DDSCAT version 5a.* Princeton Observatory Preprint POPe-695*,* Princeton University Observatory, Princeton University, Princeton, NJ, 39 pp. [Available form Princeton University Observatory, Princeton University, Princeton, NJ 08544-1001; available via anonymous ftp from astro.princeton.edu/draine/scat/ddscat/ver5a.]

32. B. T. Draine and P. J. Flatau, "Discrete-dipole approximation for scattering calculations," *J. Opt. Soc. Am . A,* **11**, pp. 1491-1499, 1994.

33. C. W. Ulbrich, "Natural variations in the analytical form of the raindrop size distribution," *J. Climate Appl. Meteor.,* **22**, pp. 1764-1775, 1983.